# Relation between Microscopic Structure and Macroscopic Properties in Polyacrylonitrile-based Lithium-Ion Polymer Gel Electrolytes

*Jeramie C. Rushing, Anit Gurung, and Daniel G. Kuroda**

Department of Chemistry, Louisiana State University, Baton Rouge, Louisiana 70803, United States

*Address correspondence to dkuroda@lsu.edu

**ABSTRACT**

Polymer gel electrolytes (PGE) have seen a renewed interest in their development because they have high ionic conductivities, but low electrochemical degradation and flammability. PGEs are formed by mixing a liquid lithium-ion electrolyte with a polymer at a sufficiently large concentration to form a gel. PGEs have been extensively studied, but the direct connection between their microscopic structure and macroscopic properties remains controversial. For example, it is still unknown whether the polymer in the PGE acts as an inert, stabilizing scaffold for the electrolyte or it interacts with the ionic components. Here, a PGE comprised of a prototypical lithium-carbonate electrolyte and polyacrylonitrile (PAN) is pursued at both the microscopic and macroscopic levels. Specifically, this study focused on describing the microscopic and macroscopic changes in the PGE at different polymer concentrations. The results indicated that the polymer-ion and polymer-polymer interactions are strongly dependent on the concentration of the polymer and the lithium salt. In particular, the polymer interacts with itself at very high PAN concentrations (10% weight) resulting in a viscous gel. However, the conductivity and dynamics of the electrolyte liquid components are significantly less affected by the addition of the polymer. The observations are explained in terms of the PGE structure, which transitions from a polymer solution to a gel, containing a polymer matrix and disperse electrolyte, at low and high PAN concentrations, respectively. The results highlight the critical role that the polymer concentration plays in determining both the macroscopic properties of the system and the molecular structure of the PGE.

## INTRODUCTION

In the last decade, lithium ion batteries have emerged as the dominant energy storage technology for most modern applications, such as portable electronics, electric vehicles, and energy storage for power grids.[1-5] However, serious safety concerns remain for the lithium ion storage technology from the use of flammable carbonate solvents in the electrolyte.[6, 7] Hence, there has been a substantial interest in developing safer alternatives. One solution to this problem is the use of polymer gel electrolytes (PGEs), wherein a non-aqueous lithium ion electrolyte is contained in a polymer matrix that stabilizes the system.[8-10] The complex composition of these electrolytes raises questions about the relationship between the molecular level interactions of the system and the macroscopic properties of the PGEs.

Previous studies have raised the question of whether the polymer in PGE acts as an inert and stabilizing scaffold for the electrolyte or alters the physical and chemical properties of the system by strongly interacting with the electrolyte. Evidence suggests that the behavior of the polymer in the PGE is directly related to the identity of the polymer, such that PGEs comprised of different polymers have different properties. Several studies have probed the macroscopic effects on the PGE for three polymers: polyethylene oxide (PEO), poly(methyl methacrylate) (PMMA), and polyacrylonitrile (PAN). In PAN-PGEs, it has been observed that the addition of polymer leads to an increase in the concentration of lithium ion pairs.[11-13] In contrast, the presence of PEO in a PGE results in more dissociated lithium salts, or equivalently a lower concentration of ion pairs, when compared to the pure organic nonaqueous electrolyte .[14, 15] Finally, for PGEs comprised of PMMA, the lithium speciation does not appear to change as a function of the polymer concentration.[16, 17] In agreement with the change in lithium speciation, the three polymers also display contrasting ionic transport behavior. For example, PMMA PGEs show that the addition of the polymer has no

impact on ion transport likely due to the lack of interactions between the lithium ions and the polymer.[12, 17-21] In contrast, PEO-PGEs present lithium conductivities that are coupled to the segmental motions of the polymer chain because the same lithium-polymer interactions that decrease the amount of contact ion pairs also enhance the coordination of lithium ions by the polymer.[22-25] Hence, PMMA and PEO appear to have opposite roles in the PGE. PMMA serves as an inert host with no impact on dynamics, PEO acts as an interacting medium in which coordination to the polymer directly impacts the flow of ions. PAN occupies a role between these two extremes, wherein the polymer interacts with the ionic components of the electrolyte, but the conductivity of the system is independent of the polymer segmental motions.[11, 20, 26, 27] Moreover, under certain conditions, it appears that the addition of PAN leads to an increase in the conductivity of the PGE, indicating that the polymer not only interacts with the electrolyte, but also plays a role in enhancing the PGE conductivity.[11] However, the molecular-level mechanism driving these changes in the PAN-PGE that lead to the enhanced conductivity is currently unknown.

From a molecular perspective, the decoupling of the diffusive behavior from the segmental motions of the polymer, observed in PMMA-PGEs, implies that the ionic motion is controlled exclusively by diffusion. However, this effect alone does not explain the observed increase in conductivity because the PGE viscosity is also increased.[20, 21] It has been proposed that the polymer enhances dissociation of the lithium salt and leads to the larger conductivity in PAN-PGE.[28] However, this hypothesis conflicts with another study, which observed that the interactions between lithium ions and nitrile groups of PAN not only enhanced the conductivity but also promoted the formation of ion pairs.[11] The role of PAN in promoting the formation of ion pairs is supported by other studies, which describe a much weaker perturbation of the anion when compared to the solvent.[13, 29, 30] Moreover, a separate Raman study showed that the polymer

enhances the ion-solvent interactions.[12] It has also been hypothesized that the lithium-polymer interaction increases conductivity because it frees the lithium from the anion, providing a molecular framework for allowing a hopping of the dissociated lithium ions along positions of the polymer backbone.[26, 29, 30] Again, this complex interpretation contradicts several studies, which have shown that the presence of PAN enhances ion pair formation and that the anions are located predominantly in the vicinity of the cation.[12, 13] Another study hypothesized that the enhanced conductivity resulted from a greater mobility of the anion rather than the cation, since the cation presents a similar transference number for several different salts due to the strong coordination to the polymer.[31] While an ion transport mechanism where the lithium ion are confined to jumping along the polymer chain and the anion moves alone[30] is possible, it conflicts with the strong solvent-polymer interactions observed in the PAN-PGEs.[16, 32-35] Other research suggests that the lithium ion interacts similarly with both the solvent and the PAN nitrile groups.[26, 29, 36] While the ability of lithium ions to associate with the polymer and the solvent can explain the increased ion mobility, their role is ambiguous and complicates the interpretation of the experimental results, creating a murky molecular picture.

The conflicting molecular models for the PGE merit further studies on the structure and dynamics in these complex systems. In this work, PGEs comprised of a lithium-ion electrolyte and different amounts of polyacrylonitrile (PAN) polymer were studied to determine the effect of polymer content on the structure and properties of the system. To this end, three different samples of electrolytes were utilized: lithium perchlorate dissolved in a mixture of cyclic carbonates (ethylene and propylene carbonate) with 0%, 5%, and 10% mass percent of PAN (Scheme 1). The microscopic properties of the system were investigated using linear and time resolved IR spectroscopies. In this case, the nitrile stretch of PAN serves as a built-in probe and has been

previously utilized to study structure in PGEs and other alkylnitriles.[13, 26, 29, 30, 37-39] However, the structure and picosecond dynamics of the PGE from the perspective of the ion were characterized using 2DIR spectroscopy in combination with lithium thiocyanate (LiSCN) as a vibrational probe. The thiocyanate ion is particularly useful for studying PGEs due to its strong infrared nitrile stretch band with a long vibrational lifetime, its small size that enables the probing of confined domains without steric hindrance, and its ionic nature that makes it remain in the high dielectric part of the system.[38, 40-44] In addition to microscopic characterization, conductivity, viscosity and differential scanning calorimetry measurements (DSC) were performed to obtain a good description of the macroscopic changes observed in the electrolytes. In particular, DSC is used to characterize the structure of polymers.[11, 33, 35, 45-47] Overall, the studies presented here allow us to derive a comprehensive molecular picture of the electrolyte as a function of the polymer concentration.

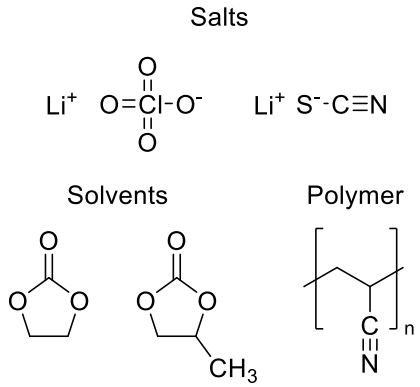


Scheme 1. Chemical structure of substances used in this stuy. From top to bottom, lithium salts: lithium perchlorate ($LiClO_4$, left) and lithium thiocyanate (LiSCN); solvents: ethylene carbonate (EC, left), propylene carbonate (PC, right); and polymer: polyacrylonitrile (PAN).

## EXPERIMENTAL METHODS

**Sample preparation.** To remove any dust or contaminants, polyacrylonitrile (PAN, Scientific Polymer Products, MW ~150,000) was dissolved in dimethylformamide, and the resulting solution was filtered with a 0.2 μm polytetrafluoroethylene filter into 18MΩ water. The polymer was then dried at 39 $^oC$ in a vacuum oven for 24 hours. Lithium perchlorate ($LiClO_4$, Aldrich) was dried at

140 ºC in a vacuum oven for 24 hours. Lithium thiocyanate hydrate ($LiSCN.xH_2O$, Alpha Aesar) was first dried in a vacuum oven under 60 °C for 1 day and then under 110 °C for 2 days. Propylene carbonate (PC, Acros Organics, 99.5%) was dried under activated 4 Å molecular sieves. Ethylene carbonate (EC, Acros Organics, 99+%) was used as received without further purification. All reagents and prepared samples were stored in a $N_2$-filled glovebox. The detailed procedure for the sample preparation can be found in the Supplementary Material. Unless otherwise noted, all the samples contained polymer concentrations between 2.5% to 15% in mass percent, while the total moles of solvent in each sample were adjusted to fulfill the following relationship of one lithium ion per 9 coordination units, where coordination units denote either the solvent or the polymer. The specific molar ratios and the weight percent of the components in the three different main samples are given in the Supplementary Material. In addition, samples containing the thiocyante ion have a concentration of ~30 mM for this anion. Sample cells utilized in FTIR and 2DIR spectroscopy consist of a PGE sample compressed between two $CaF_2$ windows with no spacer. All sample cells were prepared in a glovebox to minimize water contamination. The three electrolytes investigated here contained the lithium salt, ethylene carbonate (EC), propylene carbonate (PC) and PAN at different molar ratios. Note that the molar ratio between EC and PC as well as the molar ratio between the lithium salt and the total number of coordinating units (solvent + polymer) were kept constant across samples.

**FTIR spectroscopy.** FTIR spectra were acquired at room temperature on a Bruker Tensor 27 spectrometer having a mercury cadmium telluride (MCT) detector cooled via liquid nitrogen. Each spectrum has 0.5 $cm^{-1}$ resolution and results from an average of 40 scans. For temperature-dependent FTIR measurements, the sample was placed in a Harrick temperature-controlled sample cell directly connected to a Pharmacia Biotech circulating bath.

**Two-dimensional (2D) IR spectroscopy.** The setup used for recording 2DIR spectroscopy measurements has been described previously in the literature, so only a short summary is provided here.[48, 49] A Ti:sapphire amplifier (comprised of a Spectra Physics Mai Tai oscillator and Spitfire Ace regenerative amplifier) with a 5 kHz repetition rate was used in conjunction with an optical parametric amplifier (OPA-800C) and difference frequency generation crystal to give broadband infrared pulses. Three replica IR pulses were focused on the sample in the boxcars geometry, generating the photon echo signal in the phase matching direction $-\mathbf{k}_1 + \mathbf{k}_2 + \mathbf{k}_3$, which was subsequently overlapped with a fourth local oscillator pulse for heterodyne detection.[49] After dispersion on a Triax monochromator, the heterodyned signal was measured by a 64 element MCT array detector (Infrared Systems Development). The signal was measured with respect to three-time intervals: the coherence time $\tau$ (the separation between pulses 1 and 2), the waiting time $T_w$ (the separation between pulse 2 and 3), and the coherence time $t$ (the separation between pulse 3 and the signal). Each interval was set via computer-controlled translation stages. For each waiting time, 2DIR spectra were collected by scanning $\tau$ from -4 ps to +4 ps with a 5 fs step; both the rephrasing and non-rephasing data were collected by switching the time ordering.[49] The local oscillator always preceded the detected signal by ~0.7 ps. Spectra were collected for waiting times ranging from 0 to 100 ps in an exponential timestep (22 total steps). The time domain signal, collected as a function of ($\tau$, $T_w$, $\lambda_t$) via a monochromator-array detection, was transformed into the 2DIR spectra ($\omega_\tau$, T, $\omega_t$) via Fourier transforms, which has been thoroughly detailed elsewhere.[50] To check experimental reproducibility, the 2DIR measurements were performed in at least duplicates.

**Viscosity and conductivity measurements.** Viscosity measurements were recorded on a Brookfield DV-II+ Pro viscometer. The ionic conductivity of the PGE was measured using a

home-build conductivity meter consisting of a DFRobot conductivity probe and board controlled with Arduino microcontroller.

**DSC measurements.** DSC measurements were performed on a Discovery DSC 250 (TA Instruments) using an empty pan as reference. The samples (~10 mg) were held in hermitically sealed alodined aluminum pans, which were prepared inside a nitrogen-purged glovebox to minimize moisture contamination. The DSC samples were cooled to -40°C and equilibrated for 5 minutes before heating at a rate of 3°C per minute until 140°C. The system was purged with nitrogen at a rate of 50 mL/min.

## RESULTS

### A. Macroscopic characterization

The conductivity and viscosity of the electrolyte is presented in Table 1. Interestingly, the conductivity appears to decrease by 20% for PGE containing 5% of PAN in the electrolyte, but it remains constant at PAN concentrations of 10%. In contrast, the viscosity of the solution increases significantly with the addition of PAN. The changes in viscosity are in agreement with the macroscopic changes seen in the sample (Figure 1), where the pure electrolyte is a liquid and the addition of 5% PAN results in viscous liquid. However, the addition of 10% PAN results in a non-flowing sample, with a large viscosity, compatible with the rheology of a gel.

Table 1**.** The viscosities and conductivities of the electrolytes with various PAN concentrations at 20 °C.

| Sample | Viscosity (cP) | Conductivity (mS/cm) |
|---|---|---|
| 0% PAN | 11.9 cP | 2.1 ± 0.2 |
| 5% PAN | 2965 cP | 1.7 ± 0.2 |
| 10% PAN | ~93,000 cP | 1.7 ± 0.2 |

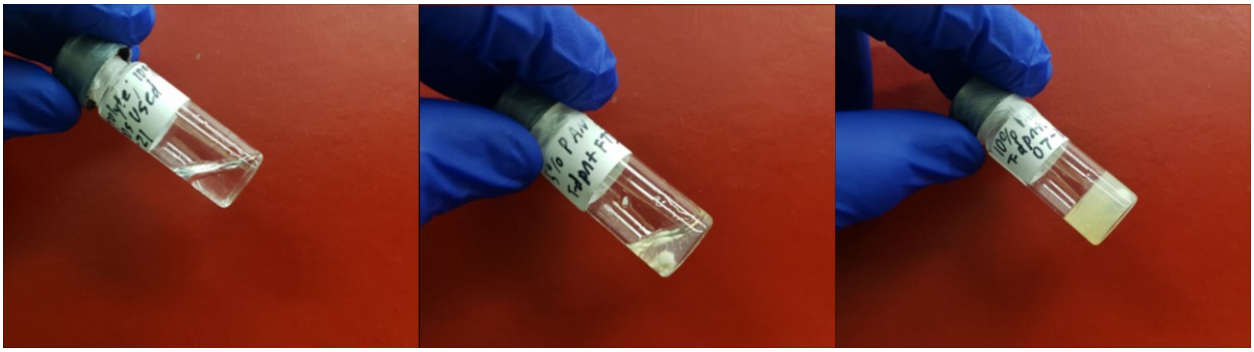

Figure 1. Images of all three samples: 0% PAN (left), 5% PAN (middle), 10% PAN (right).

The macroscopic structure of the PGEs was further investigated using modulated DSC (Figure 2). The DSC thermogram of 5% PAN-PGE shows two phase transitions in the range of 50-100°C and separated by 10°C, which are both present in the non-reversing signal, indicating that these transitions are kinetic events. In contrast, the DSC thermogram of the 10% PAN-PGE reveals three transitions at 55 ºC, 82 ºC and 92 ºC, in which the first two appear in the non-reversing signal and last one in the reversible signal. Hence, the change in the reversing heat signal at 92 ºC for the 10% PAN-PGE is associated with thermal changes. This feature is also present in the pure PAN sample at approximately the same temperature, where the phase transition corresponds to the glass transition of PAN.[45]

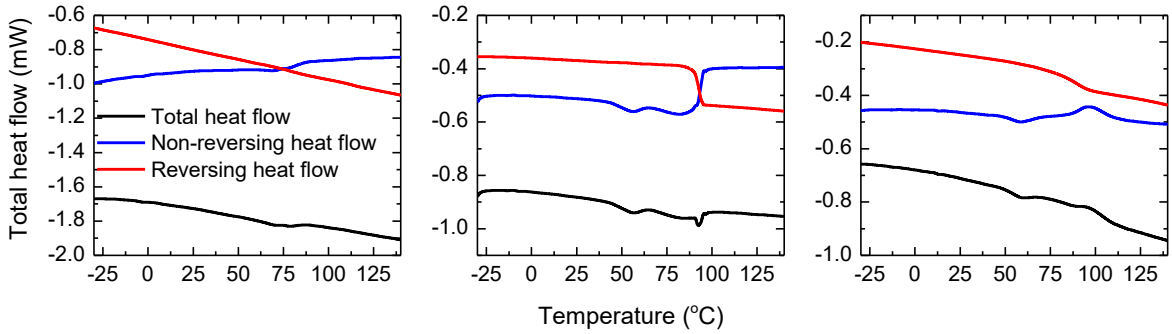


Figure 2**.** Differential scanning calorimetry results. Modulated DSC thermograms of the 5% PAN-PGE (left), 10% PAN-PGE (middle) and pure PAN (right).

## B. Microscopic characterization

The microscopic characterization was performed using IR spectroscopies. The interaction between PAN and lithium ions was confirmed using the nitrile band of PAN, where a high frequency band

appears next to the uncoordinated nitrile band of the polymer.[13, 26, 36, 51, 52] FTIR spectra for the three polymer samples containing PAN at 2.5% and three different concentrations of the lithium salt (Figure 3) show the low frequency band (2244 $cm^{-1}$) in the absence of lithium ions and the growth of a high frequency band (2270 $cm^{-1}$) with the addition of the lithium salt. While the frequency position of the two nitrile bands do not have an appreciable shift in frequency with salt concentration, the ratio of areas of the two bands varies significantly under the same conditions. At low lithium concentrations, the intensity of the high frequency band is lower than the intensity low frequency band, but this trend reverses at high lithium concentrations, since the high frequency band becomes the most intense band. These results are in agreement with previous characterization of similar PGEs.[13, 26]

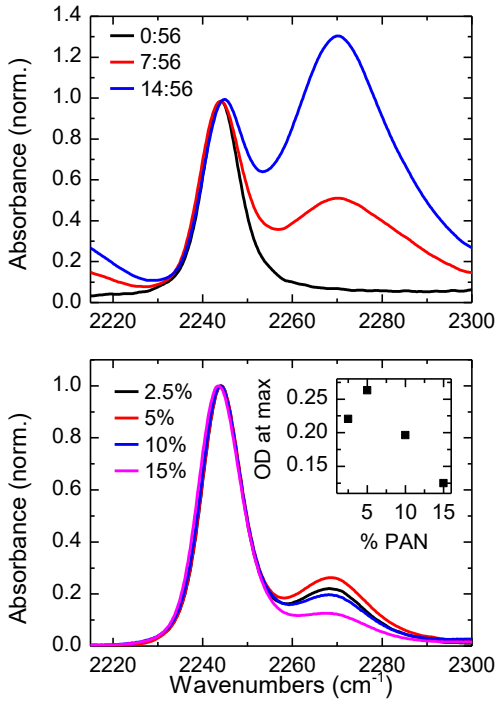


Figure 3**.** FTIR spectra of the nitrile stretch region of PAN in the PGE. Top panel shows the effect of the lithium salt concentration (at 0:56, 7:56 and 14:56 of lithium to total coordinating units) on the 2.5% PAN mixtures, while the bottom panels exhibits the effect of polymer concentration on the Li+/EC/PC mixtures from 2.5% to 15% PAN concentration. The inset on the bottom panel displays the change in the maxima of the coordinated band at 2268 $cm^{-1}$ as a function of the PAN concentration.

The changes in nitrile stretch region for the electrolyte as a function of the PAN concentration were also studied (Figure 3). To assess the coordination degree of PAN nitrile side chains, the samples contained a fix ratio of total coordination units from the solvent (EC and PC) and PAN. Each spectrum in Figure 3 shows the same two bands as in the lithium concentration dependent study, but because of low concentration of the lithium salt, the low frequency (free) band at 2244 $cm^{-1}$ remains more intense than the high frequency (lithium coordinated) band at all concentrations. Moreover, the high frequency band shows a slightly increase in intensity until PAN reaches a 5% concentration and decreases when the polymer concentration is further increased.

The molecular interactions in the PGEs from the polymer perspective were only probed using temperature dependent IR spectroscopy because the polymer nitrile groups have a low transition dipoles,[38] which combined with the scattering of the gel samples hindered the measurement of their 2DIR spectra. IR spectra as function of temperature for two PGEs (5% and 10% PAN) show that upon increasing the temperature from 5 ºC to 35 ºC, the low frequency band of PAN remains unchanged, while its high frequency band (2270 $cm^{-1}$) shows a slight red frequency shift (Figure 4). However, the intensity of high frequency band of PAN presents a different behavior for the two PGEs when the temperature is raised: increases for 5% PAN-PGE and slightly decreases for the 10% PAN-PGE.

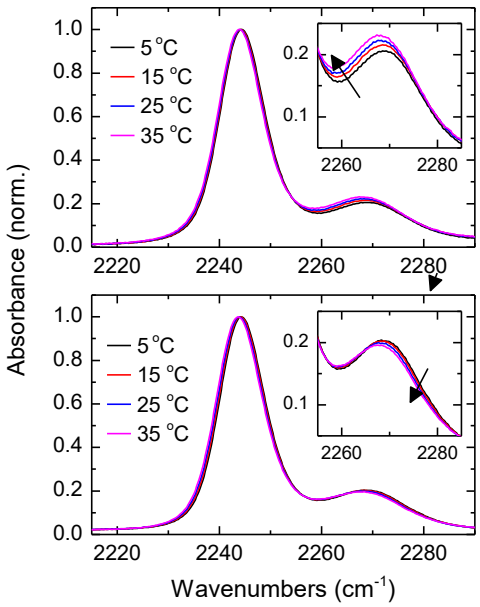


Figure 4. Temperature dependent FTIR spectra in the nitrile stretch region of PAN in PGEs. Top and bottom panels depict the 5% and 10% PAN PGEs as a function of temperature, respectively. Insets depict the changes in the coordinated bands, where the arrow indicates the direction of the change in absorption band.

The effect of the polymer on the electrolyte structure was investigated from the ion perspective using 2DIR spectroscopy and lithium thiocyanate probe. The 2DIR spectra of the samples having PAN concentrations of 0%, 5% and 10% are shown in Figure 5. For all PGEs, the 2D IR spectra exhibit two peaks: a positive (red) peak and a negative (blue) peak. The positive peak is located along the diagonal line ($\omega_\tau = \omega_t$) and arises from vibrational transitions involving both the ground ($\nu = 0$) and first excited ($\nu = 1$) states. In contrast, the negative (blue) peak appears at lower probe frequencies ($\omega_t$) because it comprises vibrational transitions from the first excited state (v=1) to the second (v=2), which are anharmonically shifted. The time evolution of the 2DIR spectra of the three samples (row in Figure 5) shows peaks that are initially elongated along the diagonal (black line where $\omega_\tau = \omega_t$), but become rounder and less elongated as waiting time progresses due to the process of spectral diffusion.[49] In particular, it is apparent that the pure electrolyte adopts a more upright peak shape at 70 ps than either sample with polymer possesses, indicating a faster dynamics of the spectral diffusion process for this sample.

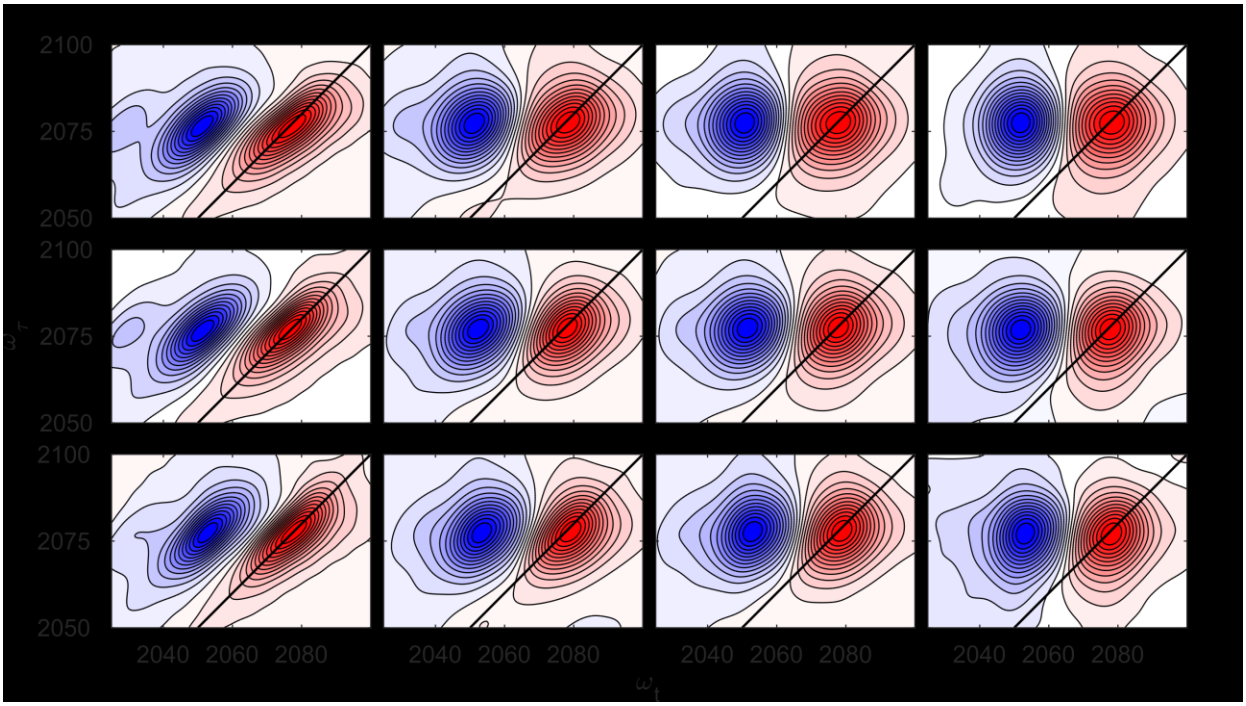

Figure 5. 2DIR spectra for thiocyanate ion in the electrolytes containing 0% (top row), 5% (middle row), and 10% (bottom row) PAN. The plotted spectra (from left to right) correspond to $T_w$ = 0ps, 10 ps, 40.2 ps, and 69.7 ps.

## DISCUSSION

### A. Microscopic interactions

The FTIR spectra in Figure 3 shows the nitrile stretch region of the polymer as a function of lithium salt concentration. Given the behavior of the nitrile bands with the addition of lithium ions, the nitrile bands are assigned to the free (low frequency at 2244 $cm^{-1}$) and lithium coordinated (high frequency at 2269 $cm^{-1}$) nitrile PAN stretches in agreement with previous assignments.[13, 26, 36, 51, 52] It is also observed from this salt concentration experiment that the concentration of lithium ions controls the degree of coordination in the polymer side chains.[29, 30, 36] However, for low ratios of lithium ions to total number of coordinated units, the linear IR spectra (Figure 3) revealed that the majority of PAN nitrile groups are free. Previous literature has noted a similar behavior for the coordination of the PAN nitrile groups upon addition of lithium salts in both Raman and FTIR

experiments, but the lack of concentrations reported therein made their comparison impossible.[13, 16, 29, 36]

The addition of PAN for fixed amounts of lithium ions shows that the number of coordinated nitrile groups does not monotonically increase with the polymer concentration. The coordinated band of PAN has a maximum intensity at 5% PAN. The presence of the maximum indicates that a polymer concentration beyond 5% does not result in more coordination of the PAN nitrile groups to cations. Note that this non-monotonic behavior in the coordination of PAN-nitrile groups has been previously reported but at higher lithium and PAN concentrations than the present study.[29] The unusual trend cannot be explained in terms of a dilution effect and likely denotes additional changes in the molecular structure in the PGEs containing 5% and 10% PAN. The differences in the PGE molecular structure are supported by the temperature-dependent FTIR spectra, where these samples show opposite trends for the coordinated band when the temperature is increased (Figure 4). Hence, the above results suggest that the polymer in the 5% PAN-PGE has a structure that can undergo structural changes that enhance the lithium-polymer interactions at high temperatures, while the 10% PAN-PGE adopts a structure that slightly diminishes the lithium-PAN interactions as the temperature is increased.

The difference in the structure of the PGEs was further derived from the DSC (Figure 2). The two transitions observed for the 5% PAN-PGE are present in the total and the non-reversing heat thermograms. Hence, these processes are assigned to kinetic processes likely arising from a greater mobility of the polymer chains due to polymer untangling at high temperature.[53] In contrast, the 10% PAN-PGE presents a large change in the reversing heat flow thermogram, which is associated with phase transtions. The same process is also present at approximately the same temperature in the pure PAN thermogram, where only melting can occur; suggesting that the melting of PAN

occurs in 10% PAN-PGE as well. The differences in the structure derived from the DSC studies of the two PGEs agree with the observations from the FTIR temperature dependence experiments. At 5% PAN concentrations, the mobility of the polymer chains is enhanced by the high temperature, which induces an increase in the coordination of the nitrile groups to lithium ions. In contrast, the change in temperature in the 10% PAN-PGE does not lead to major changes in the linear IR spectrum of the polymer because most of the PAN in the sample is found forming aggregates, in which the only the side chains at the interface of the aggregate interact with lithium ions.

The ionic probe reveals that the liquid part of the PGE does not vary significantly as a function of the polymer concentration, since the nitrile stretch of the thiocyanate ion remains almost invariant in both central frequency and bandwidth (Figure S3 in the Supplementary Material). Modeling of the nitrile stretch of the ion with a Voigt profile quantifies a small change of ~5% in the band broadening (see Table S2 in the Supplementary Material), but the width of the IR band is related to both the distribution of environments sampled by the ion and by the time that it takes to sample such a distribution.[49] Hence, the underlying cause behind the slight change of the width of the nitrile stretch band of the ion cannot be distinguished by FTIR spectroscopy and requires the use of 2DIR spectroscopy. The dynamics of the spectral diffusion process, extracted using the nodal line slope methodology,[54] shows a time dependent signal (Figure 6), which is well described with two decay times having distinct timescales. The fast motion has a characteristic time of ~3 ps, and the slow motion varies between ~30 ps for the pure electrolyte to ~70 ps for 10% PAN-PGE (Table 2 and Table S2 for full fitting parameters are in the Supplementary Material). While the spectral diffusion dynamics of the ion in the samples can be decomposed into rotational and translational contributions using the appropriate modeling,[55] the total dynamics of spectral diffusion for the

different electrolytes reveals that the ions observe a relatively smaller change in the total dynamics with increasing PAN concentration. These small changes in dynamics contrast with the drastic variations seen in the macroscopic structure of the electrolyte (i.e., liquid to a gel, Figure 1).

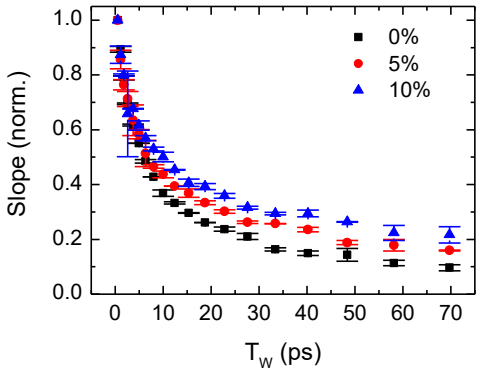


Figure 6. Slope as a function of waiting time, $T_w$ for the electrolytes containing 0% PAN (black), 5% PAN (red), and 10% PAN (blue). Duplicate measurements were used to derive the error bars in the slope analysis (see Supplementary Material).

Table 2. Characteristic times of the slope dynamics as described in the text.

| Sample | Parameters | |
|---|---|---|
| | $t_1$ (ps) | $t_2$ (ps) |
| 0% PAN | 3.1 ± 0.3 | 32 ± 3 |
| 5% PAN | 3.4 ± 0.4 | 57 ± 6 |
| 10% PAN | 3.1 ± 0.6 | 67 ± 9 |

Previously, a connection has been proposed between the time scale of the spectral diffusion and the viscosity in liquids because this dynamics measures the fundamental steps of translational diffusion.[40, 56] Hence, the ratio between viscosities should follow the ratio of spectral diffusion dynamics. However, the ratios of dynamics for the three samples (1.8 for 5% and 0%, and 1.2 for 10% and 5%) differ significantly from the ratios of their viscosities (250 for 5% and 0%, and 31 for 10% and 5%) suggesting that the total spectral diffusion dynamics of the ion is decoupled from the bulk viscosity.[18, 19, 21, 57] The lack of change in the ion dynamics is also in agreement with the conductivities of the samples, where the addition of significant amounts of polymers only

decreases their conductivity by 20%. To clarify the complex interactions leading to these results, a molecular picture is proposed in the following section.

**B. Molecular picture**

The data presented thus far shows that the amount of coordinated nitrile group of PAN is limited by the lithium concentration rather than by the polymer content. In addition, the coordination of the nitriles groups only changes marginally with temperature, and most of the polymer nitriles remain uncoordinated to lithium since only 12% of the nitriles are coordinated to lithium in a 5% PAN-PGE (see calculation details in the Supplementary Material). Moreover, the relative ratio between lithium ions and PAN nitrile groups increases with the addition of polymer, but these nitrile groups become increasingly less available to lithium ions at high polymer concentrations. Furthermore, the 5% and 10% PAN-PGEs display opposite lithium coordination behavior at high temperatures (Figure 4), since the 5% PAN-PGE shows higher coordination of lithium ions by the nitrile groups with increasing temperature, while the 10% PAN electrolyte has less lithium-nitrile interactions at higher temperatures. Finally, the ionic probe shows a lack of broadening in its nitrile band and relatively small changes in dynamics upon addition of the polymer, evidencing small structural changes in the liquid phase of the PGE. Combined, these observations indicate that lithium cations have preferential interactions with either the solvent or the perchlorate anion instead of the PAN nitrile groups, irrespective of the polymer concentration and temperature. These results are not surprising, since it has been previously shown a preferential interaction between polymer side chains and the solvent molecules over interactions between the PAN nitrile groups and lithium ions.[13, 16, 32, 34, 35] This observed preferential solvation has been rationalized in terms of the amount of free nitrile groups as well as the interaction of carbonate solvent molecules with functional groups of the polymer.[13, 33-35] The relatively small interactions between the

polymer and the ions explains why the cation can be transported through the PGE regardless of polymer concentration and coordination. However, the interaction model described so far does not account for the large changes in viscosity observed with increasing amount of polymer in the electrolyte.

The increase of PGE viscosity as a function of the PAN concentration is explained by the polymer-polymer interactions, which leads to dissolved and non-aggregated polymer chains at low PAN concentration, and a rigid and hollow polymer matrix at high PAN concentrations. This molecular picture is also supported by the DSC results, in which the 10% PAN-PGE presents a reversible process also observed in pure PAN (Figure 2). In contrast, the 5% PAN-PGE sample only has processes associated with kinetic changes from the larger mobility of the polymer sidechains. A molecular picture of the differences in structure of the electrolytes as a function of the polymer concentration is illustrated in Scheme 2. In the absence of the polymer in the electrolyte, the ions diffuse "freely" across the sample; while, at low PAN concentrations, the presence of polymer chains only slightly hinders the ion transport in the 5% sample. In contrast, the high polymer concentration in the 10% PAN-PGE leads to the formation of a polymer matrix, which has channels in which ions can travel using the liquid medium (i.e., electrolyte).

Previous modeling of PAN supports the presence of channels in PGEs. PAN has intramolecular repulsion between parallel adjacent nitriles, which forces the polymer to adopt an irregular helix that minimizes nitrile-nitrile interactions.[58, 59] Additionally, the presence of PC in a PAN sample results in a transition from a hexagonal to orthorhombic structure, which contains cavities large enough to hold solvent molecules within the polymer matrix.[33, 34] Hence, the mobility of lithium ions is through these helical tunnels and only depends on the diffusion through the liquid medium rather than on the mobility of the polymer chains.[60-62] Under these conditions, the lithium transport

is decoupled from the bulk viscosity as seen in the small changes in the spectral diffusion dynamics and conductivity as a function of the polymer concentration, or equivalent, viscosity.[19, 21] The formation of such a complex structure in the PAN-PGE is in agreement with previous studies on PMMA-PGE that showed behavior of a liquid electrolyte held in a polymer matrix at low PMMA concentration (<30% wt. PMMA). Hence, it is possible that the PAN-PGE has the same type of behavior because the solvation contribution from the nitrile groups is not very large given that lithium ion binds similarly to both EC and PAN-nitriles and there are always more carbonates than nitrile groups in the investigated PGEs.[11, 13, 16, 63] This molecular picture explains the similar dynamics and conductivities across electrolytes in spite of large changes in viscosity.

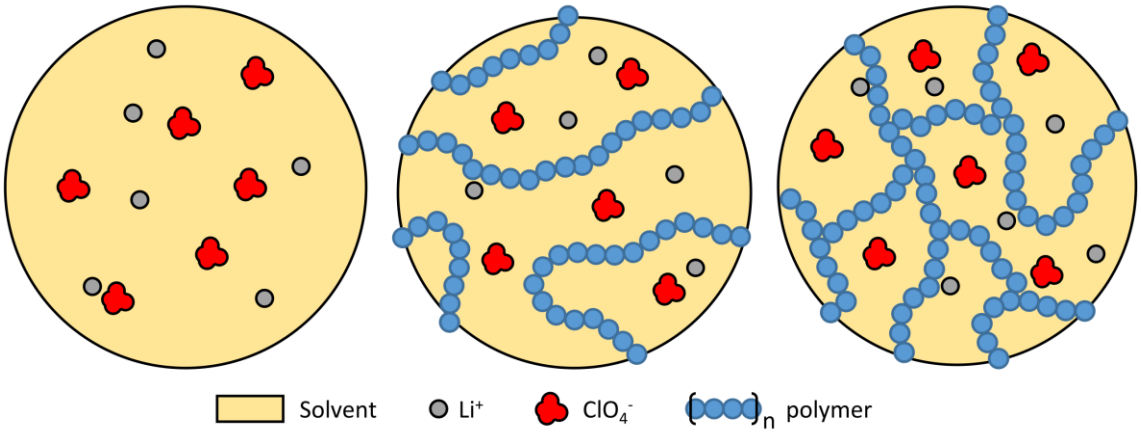


Scheme 2. Cartoon representation of the electrolyte molecular structure with PAN concentration increasing from 0% (left) to 5% (center) to 10% (right) by mass.

The proposed model also agrees with possible locations of solvent molecules described by previous research, where it was observed that cyclic carbonates are located in two different environments within PGE.[11] One environment is in the liquid medium of the gel, where the organic carbonates act as a solvent for both the polymer and the ions. The other environment is within the polymer, where the solvent is trapped in cavities formed by collapsed parts of the polymer and hence does not experience interactions with the ions.[11] Interestingly, it has been observed that the amount of solvent trapped in internal polymer cavities decreases with increasing polymer

concentration in the PGE as a result of the formation of more polymer-polymer interactions.[11] The result agrees very well with the observation made for the 10% PAN-PGE, where the lower number of solvent molecules trapped within the PAN chains and the greater amount of polymer aggregation minimizes the interactions between the lithium and the PAN nitrile group, or equivalently, maximizes the lithium interactions with carbonate molecules. In contrast, the 5% PAN-PGE has a greater number of solvent molecules trapped within the polymer chains and less polymer interacting with itself, resulting in more lithium-nitrile interactions as seen in the linear IR results (Figure 3). Additionally, several studies have indicated that among the interactions occurring in the PGE, interactions between the polymer nitrile groups and solvent molecules are favored over lithium-polymer or lithium-solvent interactions.[16, 33-35] This reflects an important consequence of the solvent confinement on the PGEs, where the lithium-polymer interactions do not depend on polymer concentration but instead on solvent confinement.

**SUMMARY**

PAN-PGEs have been characterized using microscopic and macroscopic methods, and a molecular description of the interactions in these electrolyte systems was proposed. At the macroscopic level, the viscosities of these electrolytes differed by orders of magnitude since the state of the sample drastically changes from a flowing liquid electrolyte (0% PAN) to a viscous liquid (5% PAN) to a solid gel (10% PAN) as demonstrated by the DSC thermograms; while the conductivities only showed slight declines. At the molecular level, FTIR spectroscopy revealed non-monotonic interactions between the lithium and the polymer as a function of the polymer concentration, in which low and high PAN concentrations in the PGE lead to distinct and opposite trends in the ion-polymer interaction with temperature. Moreover, a decoupling between viscosity and the dynamics of ionic components in the liquid medium of these three electrolytes is observed. These findings

were rationalized in terms of a molecular picture where PAN forms a rigid matrix at high polymer concentration, while it remains in solution when its concentration is low. In particular, the solvent appears to play a role in delaying the formation of the gel stationary phase to high polymer concentrations, because its weak interactions with the polymer hinder the interactions between polymer chains at low PAN concentrations. Hence, ion transport and its decoupling from bulk viscosity is rationalized through the presence of channels formed by the polymer in the gel, which explains its slight dependence on the polymer concentration.

## SUPPLEMENTARY MATERIAL

See supplementary material for the nitrile stretch band and its modeling for the thiocyanate ion in the different electrolytes, full fitting parameters of the spectral diffusion, and the calculation details for the percentage of coordinated nitrile groups of PAN.

## ACKNOWLEDGMENTS

The authors would like to acknowledge financial support from the National Science Foundation (CHE- 1751735) and Louisiana State University through the Economic Development Assistantship.

## AUTHOR DECLARATIONS

### Conflict of Interest

The authors have no conflicts to disclose.

### Author Contributions

Jeramie C. Rushing: Data curation (equal); Formal analysis (lead); Investigation (equal); Methodology (equal); Validation (equal); Writing - original draft (equal). Anit Gurung:

Investigation (supporting); Methodology (supporting); Validation (supporting); Writing – review & editing (supporting). Daniel G. Kuroda: Conceptualization (lead); Investigation (equal); Methodology (equal); Project administration (lead); Supervision (lead); Validation (supporting); Writing – original draft (equal).

## DATA AVAILABILITY

The data that support the findings of this study are available from the corresponding author upon reasonable request.

## REFERENCES


[1] K. E. Aifantis, S. A. Hackney, and R. V. Kumar, *High energy density lithium batteries* (Wiley Online Library, 2010),
[2] M. Armand, and J.-M. Tarascon, Nature **451**, 652 (2008).
[3] B. Dunn, H. Kamath, and J.-M. Tarascon, Science **334**, 928 (2011).
[4] K. Xu, Chem. Rev. **104**, 4303 (2004).
[5] K. Xu, Chem. Rev. **114**, 11503 (2014).
[6] G.-A. Nazri, and G. Pistoia, *Lithium batteries: science and technology* (Springer Science & Business Media, 2008),
[7] W. A. v. S. B. Scrosati, *Advances in lithium-ion batteries* (Springer Science & Business Media, 2002),
[8] X. Cheng *et al.*, Adv. Energy Mater. **8**, 1702184 (2018).
[9] K. S. Ngai *et al.*, Ionics **22**, 1259 (2016).
[10] A. M. Stephan, Eur. Polym. J. **42**, 21 (2006).
[11] P. Jayathilaka *et al.*, Solid State Ion. **156**, 179 (2003).
[12] D. Ostrovskii *et al.*, Solid State Ion. **106**, 19 (1998).
[13] D. Ostrovskii *et al.*, J. Chem. Phys. **109**, 7618 (1998).
[14] Y. Aihara, S. Arai, and K. Hayamizu, Electrochim. Acta **45**, 1321 (2000).
[15] R. Kumar, and S. Sekhon, Ionics **10**, 10 (2004).
[16] P. Johansson *et al.*, J. Phys. Chem. B **107**, 12622 (2003).
[17] D. Ostrovskii, M. Edvardsson, and P. Jacobsson, J. Raman Spectrosc. **34**, 40 (2003).
[18] O. Bohnke *et al.*, Solid State Ion. **66**, 105 (1993).
[19] H. Ericson *et al.*, Electrochim. Acta **45**, 1409 (2000).
[20] S. Panero, and B. Scrosati, J. Power Sources **90**, 13 (2000).
[21] C. Svanberg *et al.*, J. Chem. Phys. **111**, 11216 (1999).
[22] N. Karan *et al.*, Solid State Ion. **179**, 689 (2008).
[23] F. Croce *et al.*, Nature **394**, 456 (1998).
[24] F. Croce *et al.*, J. Phys. Chem. B **103**, 10632 (1999).
[25] D. Bamford *et al.*, J. Chem. Phys. **118**, 9420 (2003).

[26] B. Huang *et al.*, Solid State Ion. **91**, 279 (1996).
[27] P. Stallworth *et al.*, Solid State Ion. **73**, 119 (1994).
[28] K. Abraham, and M. Alamgir, Solid State Ion. **70**, 20 (1994).
[29] Z. Wang *et al.*, J. Electrochem. Soc. **144**, 778 (1997).
[30] Z. Wang *et al.*, Solid State Ion. **121**, 141 (1999).
[31] H. Choe *et al.*, Chem. Mater. **9**, 369 (1997).
[32] Z. Bashir, S. Church, and D. Price, Acta Polym. **44**, 211 (1993).
[33] Z. Bashir, S. Atureliya, and S. Church, J. Mater. Sci. **28**, 2721 (1993).
[34] Z. Bashir, Polymer **33**, 4304 (1992).
[35] Z. Bashir, J. Polym. Sci., Part B: Polym. Phys. **30**, 1299 (1992).
[36] Z. Wang *et al.*, Electrochim. Acta **41**, 1443 (1996).
[37] A. Ferry *et al.*, Electrochim. Acta **45**, 1237 (2000).
[38] X. B. Chen, and D. G. Kuroda, J. Chem. Phys. **153**, 164502 (2020).
[39] B. Dereka *et al.*, J. Phys. Chem. B, 278 (2021).
[40] Z. Ren *et al.*, J. Phys. Chem. Lett. **5**, 1541 (2014).
[41] Y. Cui *et al.*, Phys. Chem. Chem. Phys. **18**, 31471 (2016).
[42] A. Tamimi, H. E. Bailey, and M. D. Fayer, J. Phys. Chem. B **120**, 7488 (2016).
[43] K. Dahl *et al.*, J. Chem. Phys. **123**, 084504 (2005).
[44] S. R. G. Kankanamge, and D. G. Kuroda, Phys. Chem. Chem. Phys. **21**, 833 (2019).
[45] Z. Bashir, J. Macromol. Sci. Phys. **40**, 41 (2001).
[46] Z. Bashir, and S. Rastogi, J. Macromol. Sci. Phys. **44**, 55 (2005).
[47] M. Reading, D. Elliot, and V. Hill, in *Proceedings of the 21st North American thermal analysis society conference, Atlanta, Georgia*1992), pp. 145.
[48] M. Asplund, M. T. Zanni, and R. M. Hochstrasser, Proc. Natl. Acad. Sci. U.S.A. **97**, 8219 (2000).
[49] P. Hamm, and M. Zanni, *Concepts and methods of 2D infrared spectroscopy* (Cambridge University Press, 2011),
[50] Y. S. Kim, J. Wang, and R. M. Hochstrasser, J. Phys. Chem. B **109**, 7511 (2005).
[51] Y. Huang, and J. Koenig, Appl. Spectrosc. **25**, 620 (1971).
[52] B. Huang *et al.*, Solid State Ion. **85**, 79 (1996).
[53] L. J. Tan, A. Wan, and D. Pan, Polym. Int. **60**, 1047 (2011).
[54] K. Kwac, and M. Cho, J. Phys. Chem. A **107**, 5903 (2003).
[55] P. L. Kramer *et al.*, J. Chem. Phys. **142**, 184505 (2015).
[56] T. Brinzer, and S. Garrett-Roe, J. Chem. Phys. **147**, 194501 (2017).
[57] O. Bohnke *et al.*, Solid State Ion. **66**, 97 (1993).
[58] G. Henrici-Olive, and S. Olivé, in *Chemistry* (Springer, 1979), pp. 123.
[59] S. Rosenbaum, J. Appl. Polym. Sci. **9**, 2071 (1965).
[60] M. Armand, Solid State Ion. **9**, 745 (1983).
[61] B. Papke, M. Ratner, and D. Shriver, J. Electrochem. Soc. **129**, 1694 (1982).
[62] D. Shriver *et al.*, Solid State Ion. **5**, 83 (1981).
[63] P. Chu, and Z.-P. He, Polymer **42**, 4743 (2001).